Biochemical and Biophysical Research Communications 747 (2025) 151270

Contents lists available at ScienceDirect

Biochemical and Biophysical Research Communications

journal homepage: www.elsevier.com/locate/ybbrc

Chemical inhibition of eIF4A3 abolishes UPF1 recruitment onto mRNA encoding NMD factors and restores their expression

Chloé Mercier [a,1], Jules Durand [a,1], Annick Fraichard [a], Valérie Perez [a], Eric Hervouet [a,b], Paul Peixoto [a,b], Regis Delage-Mourroux [a], Michaël Guittaut [a,2], Aurélie Baguet [a,*,2]

[a] Université Franche-Comté, INSERM, EFS BFC, UMR1098, Interactions Hôte-Greffon-Tumeur/Ingénierie Cellulaire et Génique, F-25000, Besançon, France
[b] EPIGENExp platform, Université Franche-Comté, F-25000, Besançon, France

ARTICLE INFO

Keywords:
NMD
3′UTR
UPF1
eIF4A3
Post-transcriptional regulation
NMD autoregulation

ABSTRACT

Nonsense-Mediated mRNA Decay (NMD) is a key control mechanism of RNA quality widely described to target mRNA harbouring Premature Termination Codon (PTC). However, recent studies suggested the existence of non-canonical pathways which remain unresolved. One of these alternative pathways suggested that specific mRNA could be targeted through their 3′ UTR (Untranslated Region), which contain various elements involved in mRNA stability regulation. This study focused on 3′UTR of mRNA encoding NMD factors, on which we observed an enrichment of binding sites for UPF1 and eIF4A3 proteins, two important NMD factors. Using GFP reporter constructs containing the 3′UTR of these NMD mRNA fused to the GFP cDNA, we showed that GFP expression was significantly increased upon eIF4A3 inhibition, suggesting mRNA level stabilization. Furthermore, co-immunoprecipitation targeting UPF1 revealed that its interaction with mRNA encoding NMD factors was disrupted when cells were previously treated with the eIF4A3 inhibitor. We therefore propose that eIF4A3 might be necessary to recruit UPF1 and trigger the degradation of these transcripts through a non-canonical 3′UTR-dependent mechanism.

1. Introduction

Nonsense-Mediated mRNA Decay (NMD) is a post-transcriptional mechanism which selectively degrades transcripts harbouring a Premature Termination Codon (PTC) [1]. Recent genome-wide studies led to the estimation that about 10 % of all cellular transcripts are submitted to NMD regulation in *Homo sapiens* [2]. The canonical NMD mechanism, defined as EJC-dependent, targets mRNA either harbouring a PTC generated from alternative splicing, containing an uORF (upstream ORF), or presenting a 3′UTR with an intron [3]. NMD selectively degrades mRNA harbouring a premature termination codon (PTC) but also regulates the abundance of many cellular RNAs. The central role of NMD in the control of gene expression requires the existence of buffering mechanisms which tightly regulate the magnitude of this pathway. Here, we focused our analysis on the mechanism of NMD with an emphasis on the role of RNA helicases involved in the transition from NMD complexes recognizing a PTC to those promoting mRNA decay. We also used recent strategies to uncover novel *trans*-acting factors and their functional role in the NMD pathway. Finally, we described recent progress in the study of the physiological role of the NMD response. The EJC-dependent molecular mechanism of the NMD is fully characterized and involves two families of proteins: the UPF (Up-Frameshift) family, containing UPF1, UPF2 and UPF3B, and the SMG (Suppressor with Morphological effect on Genitalia) family, comprising SMG1, SMG5, SMG6 and SMG7. This process also requires the involvement of a multi-protein complex, called EJC (Exon-Junction Complex), deposited on the mRNA during splicing, and composed of 4 proteins (Y14/RBM8A, MAGOH, eIF4A3/DDX48 and MLN51/CASC3). While the canonical pathway is extensively detailed, little is known about the transcripts which are targeted by the NMD *via* their 3′UTR in an EJC-independent manner. Recent studies highlighted UPF1 as central in the EJC-independent NMD, hypothesis supported by its enrichment in the 3′UTR of mRNA [4]. Nevertheless, it has been reported that UPF1 can bind on non-NMD targets as well, indicating that the presence of UPF1

* Corresponding author.
E-mail address: aurelie.baguet@univ-fcomte.fr (A. Baguet).
[1] These first authors contributed equally to this work.
[2] These last authors contributed equally to this work.

https://doi.org/10.1016/j.bbrc.2024.151270
Received 17 December 2024; Accepted 30 December 2024
Available online 30 December 2024
0006-291X/© 2025 Elsevier Inc. All rights are reserved, including those for text and data mining, AI training, and similar technologies.

on a 3′UTR does not guarantee degradation by the NMD pathway [5]. One of the models proposed to explain how UPF1 might elicit NMD in an EJC-independent manner is based on the "false 3'UTR" model from yeast [6] but this model has been recently challenged thanks to the use CLIP-seq (Crosslinking and Immunoprecipitation-Sequencing) or long read nanopore sequencing and revealed that the EJC-independent NMD is not linked to the position of the stop codon and the 3′UTR length [7]. Therefore, to gain further insights into the 3′UTR-dependent mechanism targeting RNA encoding NMD factors, we identified RBP (RNA-binding protein) binding sites within their 3′UTR and we demonstrated the involvement of UPF1 and eIF4A3 proteins, operating together in a non-canonical NMD pathway.

2. Materials and methods

2.1. Cell culture and transfection

A549 cells (NSCLC, ATCC, CCL-185) were cultivated and transfected following the protocols described by Baudu et al. [8]. For RT-qPCR analysis, cells were seeded in 6-well plates (300,000 cells/well) for 24 h, transfected for 4 h with 1 μg GFP-3′UTR plasmids (Genscript), washed with Hank's buffer, and incubated for 24 h in fresh medium. For IncuCyte experiments, cells were seeded in 96-well plates (20,000 cells/well), transfected for 6 h with 500 ng GFP-3′UTR plasmids, 50 ng DsRed plasmid (transfection control), in Opti-MEM™. The medium was then replaced with DMEM containing 5 μM eIF4A3 helicase inhibitor (eIF4A3-IN-1, MedChemExpress) and incubated for further 12 h in IncuCyte live-cell imaging system (5 % CO_2, 37 °C).

2.2. RNA extraction and RT-qPCR

Total RNA was extracted using the NucleoSpin RNA Plus kit (740984.250, MACHEREY-NAGEL) and quantified with a Nanodrop. RNA was incubated with DNase (Invitrogen™ TURBO™, Thermo Fisher Scientific) at 37 °C for 30 min, followed by inactivation with EDTA (15 mM) at 75 °C for 10 min, and purified with the RNA Clean-up kit (Macherey-Nagel). Reverse transcription was performed with 100 ng of RNA using the One-Step PrimeScript™ RT-PCR Kit (Takara). For qPCR, 3 μL of 1:60 diluted cDNA, 1x TB Green Premix Ex Taq (Takara), and primers (0.1 μM) (Supplementary material) were used in a 15 μL reaction. Reactions were run on a StepOnePlus™ Real-Time PCR System and analysed using the ΔΔCT method.

2.3. IncuCyte live-cell imaging and data analysis with the SARTORIUS software

Cells were placed in IncuCyte, and 4 images per well were captured every 3 h. Analysis was performed using the Sartorius IncuCyte 2022B Rev2 software. Cell confluence was assessed using the classical confluence parameter. Green (GFP-3′UTR) and red (DsRed transfection control) fluorescence was assessed and expressed as integrated intensity/cell area per image to estimate the average amount of GFP fluorescence per cell. The time course used for the assay was chosen so that there was no significant increase in red fluorescence to avoid cell proliferation bias.

2.4. RNA immunoprecipitation (RIP)

After harvesting 20 million cells, RNA bound to UPF1 proteins was immunoprecipitated using an anti-UPF1 antibody (Cell Signaling) and Dynabeads Protein A magnetic beads (Active Motif), as described by Baudu et al. [8]. All IP steps, including bead coupling, lysis, washing, and elution, were performed using the IP-Star Compact Automated System (Diagenode) from the EPIGENExp platform. RNA was extracted from the eluate using the NucleoSpin RNA Plus kit and further concentrated with the RNA Clean-up kit (MACHEREY-NAGEL), following the supplier's recommendations. The reverse transcription was performed on purified RNA, followed by qPCR analysis with specific primers for *UPF1*, *UPF3B*, *SMG5* and *SMG7* cDNA, as described above. Reactions were run on a StepOnePlus™ Real-Time PCR System and analysed as follows: each IP UPF1 or IP IgG was reported to its corresponding input. Then each IP UPF1 to its corresponding IP IgG. The calculated Fold enrichment (IP UPF1/IP IgG) for each mRNA is then presented relative to the untreated condition.

2.5. Statistical analyses

In Fig. 1, to assess the significance of the overlap between two groups of transcripts, a statistical test was performed using the website *Statistical significance of the overlap between two groups* (http://nemates.org/MA/progs/overlap_stats.html). This website performs a hypergeometric test to assess the significance of an overlap within a larger set, for which the list of all NMD-sensitive mRNA was used. The overlap between NMD-sensitive transcripts containing, or not, an intron which bind to UPF1 and those which bind to eIF4A3 was analysed, as well as the overlap between transcripts without intron in the 3′UTR. For results presented in Figs. 2–4, statistical analyses were performed using GraphPad software (GraphPad Software Inc.). Student's t tests were used for RT-qPCR data, and ANOVA tests for IncuCyte and RIP data. All data are expressed as the mean ± SEM. *: $P \leq 0.05$; **: $P \leq 0.01$ and ***: $P \leq 0.001$.

3. Results

3.1. The 3′UTR of transcripts encoding NMD factors contain binding sites for UPF1 and eIF4A3

Since it has been suggested by Yepiskoposyan et al. that the autoregulation of transcripts encoding NMD factors could be mediated by their 3′UTR, we analysed the sequence of the 3′UTR of seven NMD transcripts (*UPF1*, *UFP2*, *UPF3B*, *SMG1*, *SMG5*, *SMG6* and *SMG7*) to search for a common pattern [9]. We compiled different information such as the size of the 3′UTR, as well as the presence or absence of an intron within the 3′UTR (Data not shown). Apart from *UPF3B*, all mRNA isoforms contain a long 3′UTR (>1000 nt). Moreover, we analysed the presence of potential RBP binding sites within the different 3′UTR of these RNA encoding NMD factors. To do so, we extracted the data regarding the binding of RBP onto the 3′UTR of RNA encoding NMD factors from the AURA database (*The Atlas of UTR Regulatory Activity*, http://aura.science.unitn.it/) which regroups CLIP-seq analyses [10]. Among the list of RBP able to interact with the 3′UTR of RNA encoding NMD factors, UPF1, FMRP and eIF4A3 bind 6 of these 3′UTR (out of 7). These observations are consistent with the statement of Kurosaki and collaborators describing that one-third of FMRP-bound mRNA are NMD targets [11]. Interestingly, we found UPF1 and eIF4A3 binding sites in all 3′UTR, apart from the one of *UPF3B*.

To assess whether eIF4A3 is commonly found on the 3′UTR of NMD-sensitive mRNA, we conducted a bioinformatic analysis combining data from the AURA database and the NMD-sensitive mRNA list characterized by Mühlemann et al. [7]. This analysis revealed 317 transcripts sensitive to NMD which were also bound by both UPF1 and eIF4A3 (Fig. 1). This list included canonical NMD substrates with introns in their 3′UTR which could be targeted by an EJC-dependent NMD, and non-canonical substrates lacking introns in their 3′UTR and therefore targeted by an EJC-independent NMD, while they were still bound by UPF1 and eIF4A3. When we sorted the transcripts by the presence or absence of an intron in the 3′UTR, we obtained a list of 242 NMD-sensitive transcripts harbouring an intron in the 3′UTR which were associated with UPF1 and eIF4A3, representing the EJC-dependent NMD targets. Interestingly, 75 NMD-sensitive transcripts (approximately 25 %) without introns were both bound by UPF1 and eIF4A3, representing the putative targets of an alternative EJC-independent NMD.

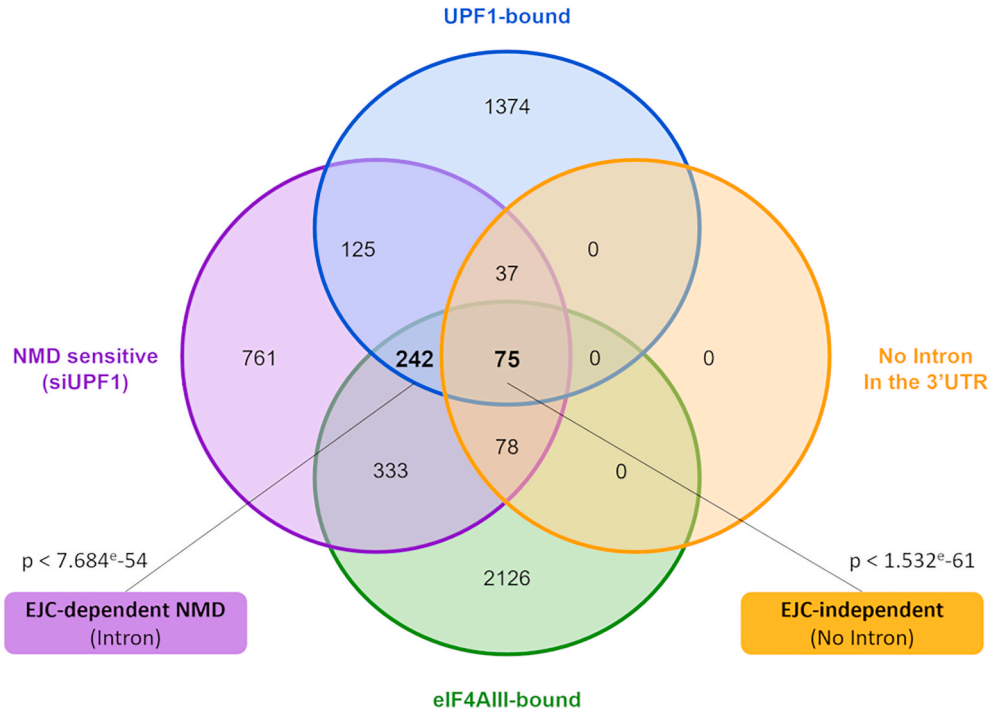

Fig. 1. Venn diagram illustrating the overlap between different mRNA groups: NMD-sensitive mRNA (purple), mRNA bound by UPF1 (blue), mRNA bound by eIF4A3 (green) and mRNA without introns (yellow). A hypergeometrical test was performed to evaluate the significance of each observed overlap between two sets within the NMD-sensitive mRNA set (see supplementary material). (For interpretation of the references to colour in this figure legend, the reader is referred to the Web version of this article.)

3.2. The 3′UTR of the transcripts encoding NMD factors regulate their expression at both RNA and protein levels

To confirm the implication of eIF4A3 in the EJC-independent NMD, we designed plasmids containing the 3′UTR of each NMD transcript cloned downstream of the GFP coding sequence in a pcDNA3.1 plasmid (Fig. 2A). Given that the 3′UTR of SMG1 was too long (4716 nt) to be successfully cloned into the plasmid, it was excluded from this study. First, we examined whether splicing events occurred within the 3′UTR of transcripts encoding NMD factors under our experimental conditions. To do so, A549 cells were transfected with the different GFP plasmids, and an RT-PCR analysis was performed using primers flanking the 3′UTR (from the end of the GFP sequence to the end of the 3′UTR). The major bands observed on gel electrophoresis corresponded to the expected size for each 3′UTR, suggesting that splicing events were rare (Fig. 2B). Then, the GFP expression obtained from these plasmids was measured at both RNA and protein levels using RT-qPCR and Incucyte (Fig. 2C and D). The transfection efficiency was assessed across all conditions thanks to the DsRed control plasmid co-transfected in all experiments (1/10 ratio compared to the GFP plasmid). It is noteworthy that we did not detect any difference in DsRed expression between the different conditions. After the transfection of the different constructions, we observed a significant decrease of GFP transcript levels when its sequence was fused to the 3′UTR of *UPF1, UPF2, SMG5, SMG6* and *SMG7* (Fig. 2C), but not when the GFP sequence was cloned before the 3′UTR of *UPF3B*. These results were consistent with those obtained for GFP fluorescence in living cells, which was significantly decreased with the 3′UTR of *UPF1, SMG5, SMG6* and *SMG7*, but not with *UPF3B* (Fig. 2D). However, we did not confirm a decrease of GFP fluorescence for the 3′UTR of *UPF2*, but this might be explained by the high variability of results between experiments for this 3′UTR.

Overall, the NMD 3′UTR which induced both a decrease of *GFP* transcript and GFP protein were those from *UPF1, SMG5, SMG6* and *SMG7* transcripts. Interestingly, these 3′UTR are characterized as long 3′UTR (>1000 nt) and we pointed out that they also contain a high number of UPF1- and eIF4A3-binding sites. In contrast, the 3′UTR of *UPF3B,* which is only 852 nt long and does not contain any UPF1 or eIF4A3 binding sites, did not induce a decrease of *GFP* transcript and protein levels. Taken together, these results suggested that eIF4A3, in collaboration with UPF1, could promote NMD in an EJC-independent manner.

3.3. Pharmacological inhibition of eIF4A3 increased GFP expression driven by the 3′UTR of NMD factors in living cells

To determine whether eIF4A3 inhibition impacted the regulation of the 3′UTR of the NMD transcripts, A549 cells were transfected with *GFP* reporters and treated, or not, with the pharmacological inhibitor of eIF4A3 helicase activity, namely eIF4A3-IN-1 (eIF4A3-IN-1, MedChemExpress). We then monitored the GFP fluorescence in living cells using IncuCyte live-cell imaging (Fig. 3). As expected, the GFP fluorescence linked to the GFP control plasmid (negative control), insensitive to the NMD, increased over time but remained unchanged between treated, and not treated conditions. We observed similar results for the plasmids containing the 3′UTR of *UPF2* and *UPF3B*. These results were consistent with the ones obtained in Fig. 2. Regarding the constructs containing the 3′UTR of *UPF1*, *SMG5*, *SMG6*, or *SMG7*, GFP levels remained low for non-treated cells, but increased significantly in the presence of the eIF4A3 inhibitor. Overall, the inhibition of eIF4A3 affected the mRNA stability and/or translation of transcripts containing the 3′UTR of *UPF1*, *SMG5*, *SMG6* and *SMG7,* but not the ones containing the 3′UTR of *UPF3B* and *UPF2*. This data supported our hypothesis that eIF4A3 was indeed involved in the regulation of NMD transcript stability and/or translation through their 3′UTR, even if these 3′UTR did not contain any EJC.

3.4. The binding of UPF1 onto the NMD transcripts is abolished by the eIF4A3 inhibition

To determine whether eIF4A3 inhibition impacted the binding of UPF1 onto mRNA encoding NMD factors, we performed RNA-IP

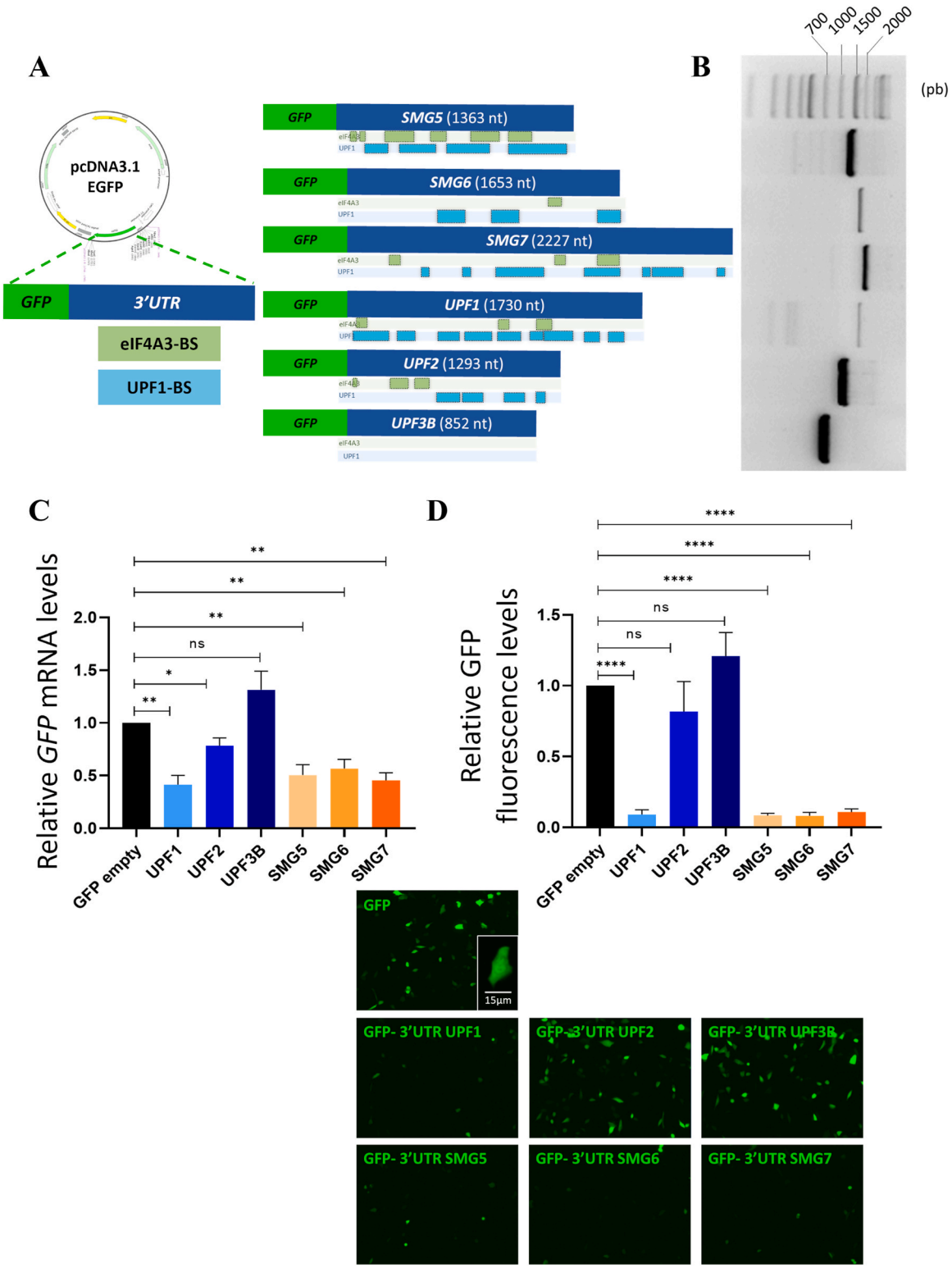

Fig. 2. Measurement of GFP transcript and protein expression driven by the 3′UTR of NMD transcripts. (A) Schematic representation of plasmid constructs used for the study of the regulation of GFP expression regulation *via* the 3′UTR of NMD transcripts. **(B)** Agarose gel electrophoresis of RT-PCR products derived from GFP-3′UTR mRNA in transfected A549 cells. The 3′UTR of the NMD transcripts *UPF1, UPF2, UPF3B, SMG5, SMG6* and *SMG7* were cloned downstream of the GFP coding sequence in a pcDNA3.1 plasmid. The empty GFP plasmid was used as a negative control of NMD degradation. **(C)** Cells were transfected for 4 h, and mRNA levels were quantified using RT-qPCR. The values were calculated using the ΔΔCT method, normalized to the housekeeping gene *18S RNA*. **(D)** Cells were transfected for 12 h with GFP-3′UTR constructs, and GFP expression was analysed by IncuCyte live-cell imaging and fluorescence GFP was quantified at 12 h using the SARTORIUS software. Data are represented as mean ± SEM of three independent experiments. P-values were calculated using the Student's *t*-test. ns: not significant, *: $p \leq 0.05$, **: $p \leq 0.01$ and ****: $p \leq 0.0001$.

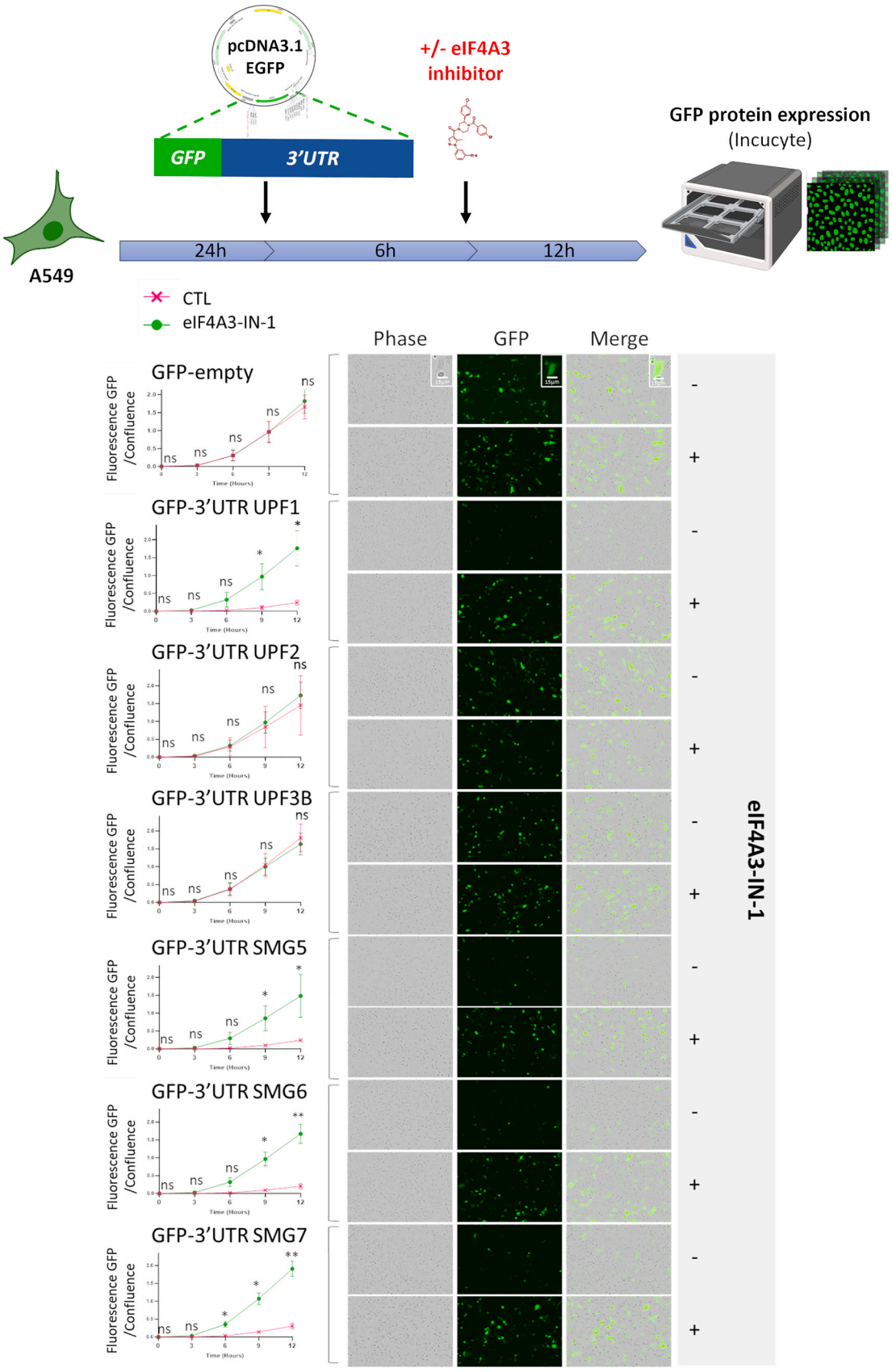

Fig. 3. Measurement of GFP expression driven by the 3′UTR of NMD transcripts in living cells, treated or not with eIF4A3-IN-1. Cells were transfected with the different GFP-3′UTR constructions and 6 h after transfection, they were treated or not, with an inhibitor of eIF4A3 helicase activity, eIF4A3-IN-1, for 12 h. GFP levels were then analysed by IncuCyte live-cell imaging and GFP fluorescence levels were quantified using the SARTORIUS software. Data are represented as mean ± SEM of three independent experiments. P-values were calculated using the Student's *t*-test. ns: not significant, *: $p \leq 0.05$, **: $p \leq 0.01$ and ****: $p \leq 0.0001$.

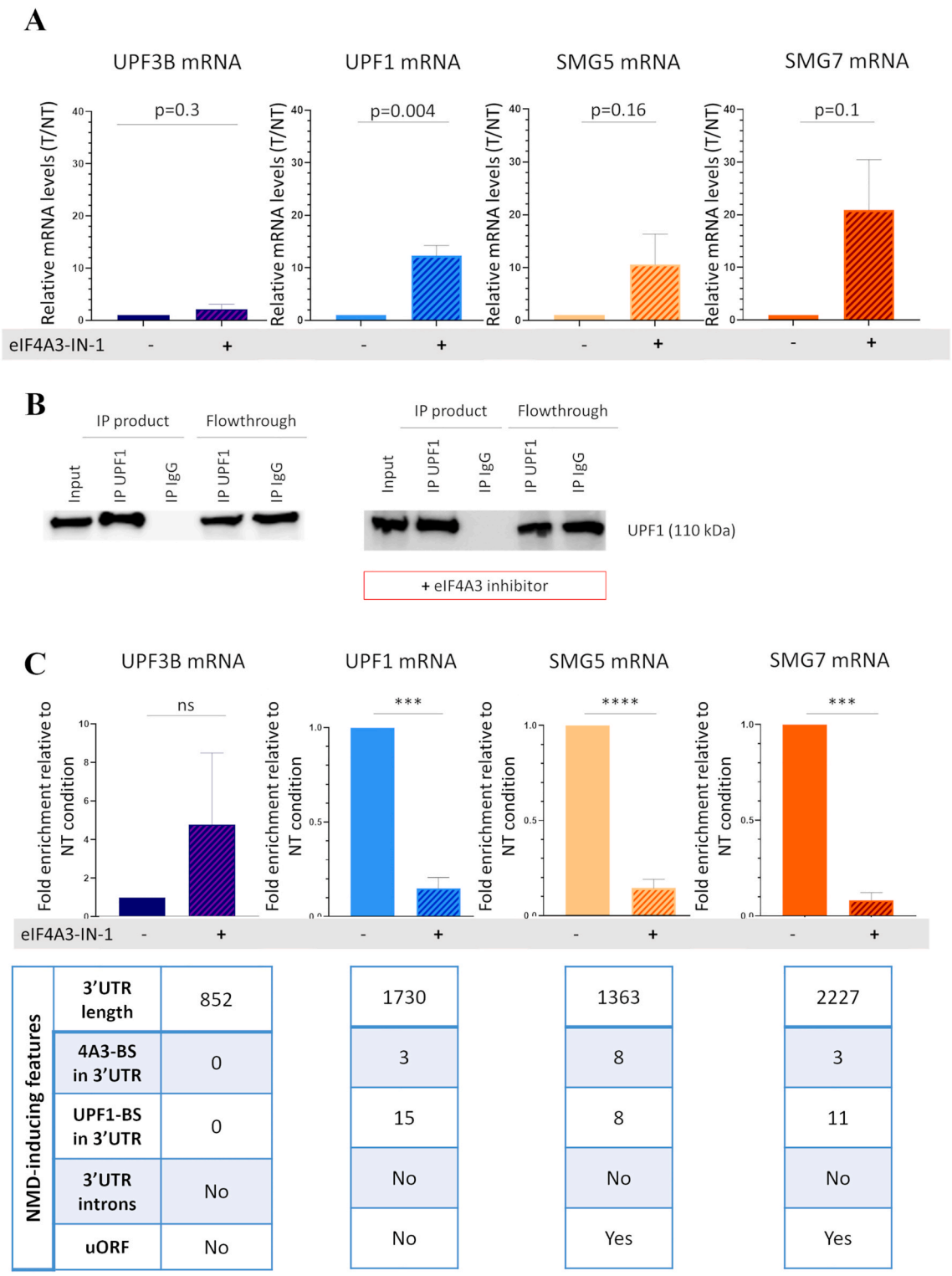

NMD-inducing features					
	3'UTR length	852	1730	1363	2227
	4A3-BS in 3'UTR	0	3	8	3
	UPF1-BS in 3'UTR	0	15	8	11
	3'UTR introns	No	No	No	No
	uORF	No	No	Yes	Yes

Fig. 4. Analysis of the enrichment of mRNA bound to the UPF1 protein by RNA immunoprecipitation (RNA IP). (A) Cells were transfected for 6 h, and mRNA levels were quantified using RT-qPCR. The values were calculated using the ΔΔCT method, normalized to the housekeeping gene *18S RNA*. **(B)** Western-Blotting performed to confirm that the addition of the eIF4A3 inhibitor did not alter UPF1 immunoprecipitation. **(C)** Total RNA from 10 million A549 cells treated, or not, with the eIF4A3 inhibitor for 6 h were collected for RNA IP. The RNA immunoprecipitated with UPF1 were then quantified by RT-qPCR using *UPF3B, UPF1, SMG5* or *SMG7* primers (blue histograms). The values were calculated using the ΔΔCT method, firstly normalized to the Input and then to the IP-IgG. Data are represented as mean ± SEM of three independent experiments. P-values were calculated using the Anova test. ns: not significant, *: $p \leq 0.05$, **: $p \leq 0.01$ and ****: $p \leq 0.0001$. (For interpretation of the references to colour in this figure legend, the reader is referred to the Web version of this article.)

experiments using an anti-UPF1 (RIP-UPF1), or a control IgG (RIP-IgG), from A549 cells treated, or not, with the inhibitor of eIF4A3 (Fig. 4). The transcripts analysed in these experiments were those containing binding sites for UPF1 and eIF4A3 (*UPF1*, *SMG5*, and *SMG7*) and the *UPF3B* mRNA, as a control (no binding sites for UPF1 and eIF4A3). First, we analysed the effect of the eIF4A3-IN-1 inhibitor on the RNA levels of NMD factors (*UPF3B, UPF1, SMG5* and *SMG7*) using RT-qPCR. The inhibitor led to an overall increase in the RNA levels of *UPF1, SMG5* and *SMG7*, whereas no significant effect was observed for *UPF3B* (Fig. 4A). We then confirmed, by western blotting, that the addition of the inhibitor did not modify the immunoprecipitation rate of UPF1 (Fig. 4B). On one hand, RNA-IP experiments showed that *UPF3B* was undetected in both the RIP-IgG and RIP-UPF1 samples and that there was no significant difference before, or after, treatment with the eIF4A3 inhibitor. Contrary to the GFP reporter experiments (Fig. 3) which focused only on the 3′UTR of the transcripts, RNA-IP data confirmed that the endogenous *UPF3B* transcript was not targeted by UPF1 (Fig. 4C). These data are consistent with the fact that *UPF3B* lacks binding sites for UPF1 and eIF4A3, and that it does not contain any uORF. On the other hand, we confirmed that the *UPF1*, *SMG5* and *SMG7* transcripts were enriched in the UPF1-IP compared to the control IgG-IP. More interestingly, when we added the eIF4A3 inhibitor, we lost the interaction between UPF1 and these transcripts since we did not detect any enrichment anymore in the UPF1-IP compared to the IgG-IP (Fig. 4C). These results demonstrated that the inhibition of eIF4A3 activity abolished the binding of UPF1 to endogenous *UPF1, SMG5* and *SMG7* mRNA, and therefore suggested that this interaction may be mediated by eIF4A3. This observation is particularly important for the *UPF1* transcript, which contains no uORF or intron in its 3′UTR, suggesting that it could be targeted by eIF4A3 to recruit UPF1 and trigger EJC-independent NMD.

4. Discussion

In this study, we analysed the 3′UTR of mRNA encoding NMD factors and demonstrated that they were enriched for UPF1 and eIF4A3 binding sites. Interestingly, we observed that these binding sites were also present on transcripts lacking introns in their 3′UTR, indicating the absence of EJC. These first results suggested that UPF1 and eIF4A3 could function together, independently of an EJC, to mediate mRNA decay. Yepiskoposyan et al. previously demonstrated that the 3′UTR of *UPF1, SMG5 and SMG7* mRNA are the main NMD-inducing features of these transcripts [9]. According to these data, using GFP reporters, we observed that the 3′UTR of *UPF1, SMG5, SMG6* or *SMG7* alone would be sufficient to decrease both the *GFP* RNA and protein levels from plasmids containing each 3′UTR cloned downstream of the *GFP* coding sequence. Interestingly, we demonstrated that pharmacological inhibition of eIF4A3 completely restored GFP fluorescence in living cells. We verified the presence of splicing events by amplifying the 3′UTR using RT-PCR and observed that the predominant signal corresponded to the expected one. However, we also detected lower bands of weak intensity, indicating that splicing events might occur for a small proportion of these transcripts. Altogether, our results suggested that eIF4A3 regulated RNA encoding NMD factor levels through their 3′UTR, even in the absence of an EJC. Then, the RNA-IP experiments demonstrated that eIF4A3 helicase activity was essential for the binding of UPF1 onto *UPF1, SMG*5 and *SMG7* mRNA.

One remaining critical question is how to explain the different regulation of the 3′UTR recognized by UPF1 and eIF4A3? It has been reported, using CLIP-seq of eIF4A3, that while most of eIF4A3 was enriched in the coding sequence, more than a half was also present in the 3′UTR [12]. This distribution suggested that the 3′UTR probably contained elements able to recruit eIF4A3 independently of the presence of an EJC. To explain how this EJC-independent NMD could work, several non-exclusive hypotheses have been proposed, such as the recruitment of eIF4A3 thanks: i) to secondary structures in the 3′UTR, or the existence of ii) G/C-rich regions and/or iii) UPF1 binding sites. This process would depend on GC-rich sequences forming stable secondary RNA structures that would serve as recognition elements for RNA-binding proteins such as UPF1 and eIF4A3. Indeed, it was further reported that highly structured transcripts generally present shorter half-lives, highlighting the role for secondary structures in transcript stability and degradation [13,14].

In addition, it has been demonstrated that UPF1 binding sites are highly sensitive to form secondary RNA structures [15,16]. RNA proximity ligation methods, such as hiCLIP (hybrid individual-nucleotide resolution UV crosslinking and immunoprecipitation) developed to study RNA duplexes bound to RBP, also revealed the *in vivo* presence of RNA duplexes in the long 3′UTR and their involvement in their degradation [17,18].

Based on these observations, we therefore propose that eIF4A3 might play an important role in the regulation of RNA encoding NMD factors, potentially by facilitating the recruitment of UPF1 onto their 3′UTR. This cooperation between two helicases, eIF4A3 and UPF1, would specifically target highly structured transcripts with long 3′UTR to facilitate their degradation. To conclude, our study suggested a coordinated action of eIF4A3 and UPF1 on 3′UTR to further induce the degradation of targeted mRNA, particularly those encoding NMD factors, and therefore indicating that eIF4A3 is important for the autoregulation of NMD.

CRediT authorship contribution statement

Chloé Mercier: Investigation, Methodology, Validation, Writing – original draft. **Jules Durand:** Investigation, Methodology, Validation, Visualization, Writing – original draft. **Annick Fraichard:** Investigation, Methodology, Supervision, Validation, Writing – original draft. **Valérie Perez:** Investigation. **Eric Hervouet:** Writing – review & editing. **Paul Peixoto:** Writing – review & editing. **Regis Delage-Mourroux:** Writing – review & editing. **Michaël Guittaut:** Conceptualization, Data curation, Funding acquisition, Investigation, Methodology, Project administration, Supervision, Writing – original draft. **Aurélie Baguet:** Conceptualization, Data curation, Investigation, Methodology, Supervision, Writing – original draft.

Declaration of competing interest

The authors declare that they have no known competing financial interests or personal relationships that could have appeared to influence the work reported in this paper.

Acknowledgements

Chloé Mercier and Jules Durand were supported by a fellowship from the MESR “Ministère de l’Enseignement Supérieur et de la Recherche.” This work was supported by fundings from Ligue Contre le Cancer (CCIR Est 2020, CCIR Est 2021 and CCIR Est 2024), INSERM, EFS BFC, Univ. Bourgogne Franche-Comté and the “Région Bourgogne Franche-Comté” (Convention Amorçage 2021Y-08309). We thank the DIMAcell platform for their technical support during Incucyte experiments. We thank Dr. Mühlemann and collaborators for sending us supplementary data from their previous publication.

Appendix A. Supplementary data

Supplementary data to this article can be found online at https://doi.org/10.1016/j.bbrc.2024.151270.

References

[1] O. Isken, L.E. Maquat, Quality control of eukaryotic mRNA: safeguarding cells from abnormal mRNA function, Genes Dev. 21 (2007) 1833–3856, https://doi.org/10.1101/gad.1566807.

[2] T. Kurosaki, M.W. Popp, L.E. Maquat, Quality and quantity control of gene expression by nonsense-mediated mRNA decay, Nat. Rev. Mol. Cell Biol. 20 (2019) 406–420, https://doi.org/10.1038/s41580-019-0126-2.
[3] N. Hug, D. Longman, J.F. Cáceres, Mechanism and regulation of the nonsense-mediated decay pathway, Nucleic Acids Res. 44 (2016) 1483–1495, https://doi.org/10.1093/nar/gkw010.
[4] D. Lavysh, G. Neu-Yilik, UPF1-Mediated RNA decay—danse macabre in a cloud, Biomolecules 10 (2020) 999, https://doi.org/10.3390/biom10070999.
[5] T. Kurosaki, L.E. Maquat, Rules that govern UPF1 binding to mRNA 3′ UTRs, Proc. Natl. Acad. Sci. U. S. A. 110 (2013) 3357–3362, https://doi.org/10.1073/pnas.1219908110.
[6] P.V. Ivanov, N.H. Gehring, J.B. Kunz, M.W. Hentze, A.E. Kulozik, Interactions between UPF1, eRFs, PABP and the exon junction complex suggest an integrated model for mammalian NMD pathways, EMBO J. 27 (2008) 736–747, https://doi.org/10.1038/emboj.2008.17.
[7] E.D. Karousis, F. Gypas, M. Zavolan, O. Mühlemann, Nanopore sequencing reveals endogenous NMD-targeted isoforms in human cells, Genome Biol. 22 (2021) 223, https://doi.org/10.1186/s13059-021-02439-3.
[8] T. Baudu, C. Parratte, V. Perez, M. Ancion, S. Millevoi, E. Hervouet, A. Peigney, P. Peixoto, A. Overs, M. Herfs, A. Fraichard, M. Guittaut, A. Baguet, The NMD pathway regulates GABARAPL1 mRNA during the EMT, Biomedicines 9 (2021) 1302, https://doi.org/10.3390/biomedicines9101302.
[9] H. Yepiskoposyan, F. Aeschimann, D. Nilsson, M. Okoniewski, O. Mühlemann, Autoregulation of the nonsense-mediated mRNA decay pathway in human cells, RNA 17 (2011) 2108–2118, https://doi.org/10.1261/rna.030247.111.
[10] E. Dassi, A. Re, S. Leo, T. Tebaldi, L. Pasini, D. Peroni, A. Quattrone, Aura 2, Translation (Austin) 2 (2014) e27738, https://doi.org/10.4161/trla.27738.
[11] T. Kurosaki, N. Imamachi, C. Pröschel, S. Mitsutomi, R. Nagao, N. Akimitsu, L. E. Maquat, Loss of the fragile X syndrome protein FMRP results in misregulation of nonsense-mediated mRNA decay, Nat. Cell Biol. 23 (2021) 40–48, https://doi.org/10.1038/s41556-020-00618-1.
[12] J. Saulière, V. Murigneux, Z. Wang, E. Marquenet, I. Barbosa, O. Le Tonquèze, Y. Audic, L. Paillard, H.R. Crollius, H. Le Hir, CLIP-seq of eIF4AIII reveals transcriptome-wide mapping of the human exon junction complex, Nat. Struct. Mol. Biol. 19 (2012) 1124–1131, https://doi.org/10.1038/nsmb.2420.
[13] J.-D. Beaudoin, E.M. Novoa, C.E. Vejnar, V. Yartseva, C.M. Takacs, M. Kellis, A. J. Giraldez, Analyses of mRNA structure dynamics identify embryonic gene regulatory programs, Nat. Struct. Mol. Biol. 25 (2018) 677–686, https://doi.org/10.1038/s41594-018-0091-z.
[14] Z. Su, Y. Tang, L.E. Ritchey, D.C. Tack, M. Zhu, P.C. Bevilacqua, S.M. Assmann, Genome-wide RNA structurome reprogramming by acute heat shock globally regulates mRNA abundance, Proc. Natl. Acad. Sci. U. S. A. 115 (2018) 12170–12175, https://doi.org/10.1073/pnas.1807988115.
[15] F. Fiorini, D. Bagchi, H. Le Hir, V. Croquette, Human Upf1 is a highly processive RNA helicase and translocase with RNP remodelling activities, Nat. Commun. 6 (2015) 7581, https://doi.org/10.1038/ncomms8581.
[16] J.A. Hurt, A.D. Robertson, C.B. Burge, Global analyses of UPF1 binding and function reveal expanded scope of nonsense-mediated mRNA decay, Genome Res. 23 (2013) 1636–1650, https://doi.org/10.1101/gr.157354.113.
[17] Y. Sugimoto, A.M. Chakrabarti, N.M. Luscombe, J. Ule, Using hiCLIP to identify RNA duplexes that interact with a specific RNA-binding protein, Nat. Protoc. 12 (2017) 611–637, https://doi.org/10.1038/nprot.2016.188.
[18] A.M. Chakrabarti, I.A. Iosub, F.C.Y. Lee, J. Ule, N.M. Luscombe, A computationally-enhanced hiCLIP atlas reveals Staufen1-RNA binding features and links 3′ UTR structure to RNA metabolism, Nucleic Acids Res. 51 (2023) 3573–3589, https://doi.org/10.1093/nar/gkad221.